

Probing fragment-capture mechanism in ${}^7\text{Li}+{}^{93}\text{Nb}$ reaction

S. K. Pandit^{1,2,*}, A. Shrivastava^{1,2}, K. Mahata^{1,2}, V. V. Parkar¹, R. Palit³,
P. C. Rout^{1,2}, K. Ramachandran¹, S. Bhattacharya⁴, V. Nanal³,
A. Kumar¹, S. Biswas³, S. Saha³, J. Sethi³, P. Singh³, and S. Kailas¹

¹Nuclear Physics Division, Bhabha Atomic Research Centre, Mumbai - 400085, India

²Homi Bhabha National Institute, Anushaktinagar, Mumbai - 400094, India

³DNAP, Tata Institute of Fundamental Research, Mumbai - 400005, India and

⁴Variable Energy Cyclotron Centre, Kolkata - 700064, India

Exploring the reaction dynamics involving weakly-bound stable/unstable nuclei is a topic of current interest [1?, 2]. Presence of loosely bound cluster structure and exotic shapes in these nuclei leads to new reaction channels, e.g., breakup, transfer-breakup, and fragment-capture. These channels contribute to a significant part of the total reaction cross sections around the Coulomb barrier energies [4–7]. Another interesting observation is the large inclusive α -particle production cross sections in reaction involving weakly bound projectiles with $\alpha + x$ cluster structure, e.g. ${}^6,{}^8\text{He}$, ${}^6,{}^7\text{Li}$, and ${}^7,{}^9\text{Be}$, compared to that of the complementary fragments. In our earlier work, we have shown that, t -capture process, which is the admixture of two processes, t -fusion after the breakup of ${}^7\text{Li}$ and direct t -stripping, is the dominant mechanism for the production of large α -yields [9]. In the present investigation, we have aimed to quantify the relative importance of the breakup-fusion and direct cluster-stripping channels.

Particle- γ coincidence experiment was performed at $E_{\text{beam}} = 24$ MeV for ${}^7\text{Li}+{}^{93}\text{Nb}$ system at Pelletron-Linac facility, Mumbai. Self-supporting ${}^{93}\text{Nb}$ foil of thickness ~ 1.75 mg/cm² was used as target. Indian National Gamma Array (INGA) was used for the measurements of prompt γ -ray transitions. All the detectors were arranged in a spherical geometry with three detectors at 23°, six detectors at 40°, five detectors at 65°, and four detectors at 90° with respect to the beam direction.

*Electronic address: sanat@barc.gov.in

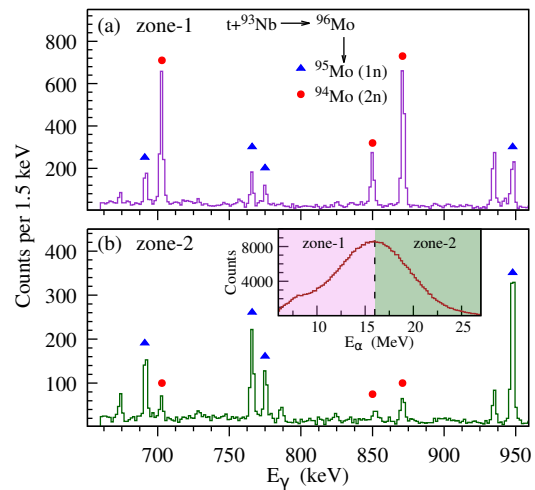


FIG. 1: A typical in-beam γ -ray spectrum in coincidence with α particle selected as the outgoing fragment for the ${}^7\text{Li}+{}^{93}\text{Nb}$ reaction at $E_{\text{beam}} = 24$ MeV. The characteristic γ -transitions from ${}^{95}\text{Mo}$ and ${}^{94}\text{Mo}$ formed due to t -capture followed by evaporation of one and two neutrons are marked.

The distance from the target to crystal was 25 cm. Efficiency and energy calibration of the clover detectors were carried out using standard calibrated ${}^{152}\text{Eu}$ and ${}^{133}\text{Ba}$ γ -ray sources. The overall photo peak efficiency was found to be around 2% at $E_\gamma = 1$ MeV. Three Si surface barrier telescopes were placed inside the scattering chamber at 35°, 45° and 70° for the detection of charged particles around the grazing angle. Thicknesses of the ΔE and E detectors were ~ 15 -30 μm and ~ 300 -5000 μm , respectively. One Si surface barrier detector of thickness ~ 300 μm was kept at 20° to monitor Rutherford scattering for absolute

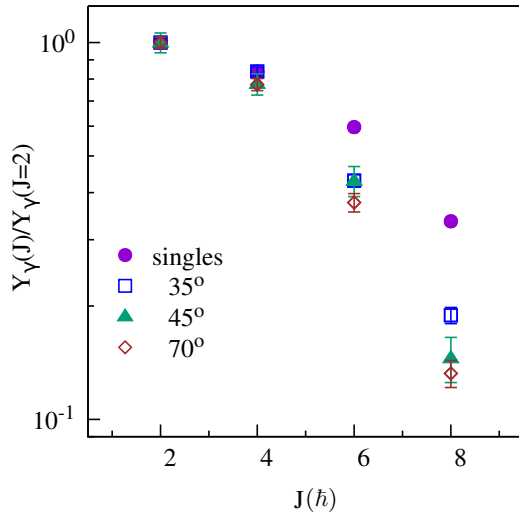


FIG. 2: The side-feeding pattern for ^{94}Mo measured in singles and in coincidence with the α -particle scattered at angles 35° , 45° , and 70° .

normalization purposes. Digital data acquisition system with a sampling rate of 100 MHz was used to collect the data in time stamped mode [8].

The fragment-capture reaction mechanism was identified by measuring prompt γ -rays arising from the residue in coincidence with the outgoing particles. The measured in-beam γ -transitions in coincidence with outgoing α -particle is shown in Fig. 1. The photo-peaks corresponding to the characteristic γ -rays from ^{95}Mo and ^{94}Mo formed due to t -capture followed by evaporation of one and two neutrons are labeled. The measured singles α -particle spectra is shown in the inset of the Fig. 1(b). Two zones, high and low energy regions of E_α are highlighted in the inset figure. The Fig. 1 (a) and (b) are corresponding to the high and low energy zone of the E_α . As can be seen from the figure the photo peaks due to γ -transitions from the residues corresponding to the two neutrons evaporation channel (^{94}Mo) are dominant for coincident α -particle with relatively lower energies (zone-1). While those from ^{95}Mo , formed after one neutron evaporation, are dominant in the zone-2 with relatively higher energy of the outgoing α -particles.

The relative intensity of the various low lying levels in ^{94}Mo from singles measurement and in coincidence with the α -particle scattered at angles 35° , 45° , and 70° are presented in Fig. 2 as a function of their spin. The trend of the data found to similar for $^7\text{Li}+^{165}\text{Ho}$ system [10]. The relative intensity found to decrease for the levels of higher spins in coincidence with the α -particles with respect to the intensity measured in singles. It can also be noticed from the figure that the slope of the falling of relative intensity increases with the scattering angle of the outgoing α -particles for higher J -values. From the present exclusive measurement of charged particle and γ -rays combined with exclusive measurements of charged particles from Ref. [5] along with theoretical calculations, the two mechanisms breakup-fusion and cluster-stripping are segregated. The details of the investigations will be presented in the conference.

We thank Mumbai Pelltron-Linac accelerator staff for providing steady and uninterrupted beam.

References

- [1] L. F. Canto *et al.*, Phys. Rep. **596**, 1 (2015); L. F. Canto *et al.*, Phys. Rep. **424**, 1 (2006).
- [2] N. Keeley *et al.*, Prog. Part. Nucl. Phys. **63**, 396 (2009).
- [3] K. J. Cook *et al.*, Phys. Rev. Lett. **122**, 102501 (2019).
- [4] A. Shrivastava *et al.*, Phys. Lett. B **633**, 463 (2006).
- [5] S. K. Pandit *et al.*, Phys. Rev. C **93**, 061602 (2016).
- [6] A. Shrivastava *et al.*, Phys. Lett. B **718**, 931 (2013).
- [7] S. K. Pandit *et al.*, Phys. Rev. C **100**, 014618 (2019).
- [8] R. Palit *et al.*, Nucl. Instrum. Methods Phys. Res., Sect. A **680**, 90 (2012).
- [9] S. K. Pandit *et al.*, Phys. Rev. C. **93**, 044616 (2017)
- [10] V. Tripathi *et al.*, Phys. Rev. C. **72**, 017601 (2005)